# *Drosophila* growth cones: a genetically tractable platform for the analysis of axonal growth dynamics

Running title
***Drosophila* growth cones**

Natalia Sánchez-Soriano*[1)], Catarina Gonçalves-Pimentel*[1) 2)], Robin Beaven[1)], Ulrike Haessler[3)], Lisa Ofner[4)], Christoph Ballestrem, Andreas Prokop[5)]

*) contributed equally

1) Faculty of Life Sciences, Wellcome Trust Centre for Cell-Matrix Research, Michael Smith Building, Oxford Road, Manchester M13 9PT, UK
2) PhD Programme in Experimental Biology and Biomedicine, Center for Neuroscience and Cell Biology, University of Coimbra, 3004-517, Coimbra, Portugal.
3) current address: current address: Institute of Bioengineering, School of Life Sciences, École Polytechnique Fédérale de Lausanne (EPFL), 1015 Lausanne, Switzerland
4) current address: Laboratory of Experimental and Molecular Hepatology, Dept. of Internal Medicine, Medical University of Graz, Auenbruggerplatz 15, A-8036 Graz
5) author for correspondence: +44-(0)161-27-51556/7, Andreas.Prokop@manchester.ac.uk

**Acknowledgements**

We are grateful to Buzz Baum, Tom Millard, David Van Vactor, Florence Janody, Jozsef Mihaly, Peter Kolodziej, E. Martin-Blanco and the Bloomington Stock Centre for providing fly stocks and antibodies. We would like to thank Melanie Klein for general assistance and Tom Millard for constructive comments on the manuscript. This work was funded through grants by the Wellcome Trust to AP, CB and NSS (077748/Z/05/Z), of the BBSRC (BB/C515998/1) to AP, a studentship from the Fundação para a Ciência e a Tecnologia to CGP (SFRH/BD/15891/2005), and EU Marie-Curie studentships to UH and LO (QLK6-CT-1999-50412). The Bioimaging Facility microscopes used in this study were purchased with grants from BBSRC, The Wellcome Trust and the University of Manchester Strategic Fund.

## Abstract

The formation of neuronal networks, during development and regeneration, requires outgrowth of axons along reproducible paths towards their appropriate postsynaptic target cells. Axonal extension occurs at growth cones at the tips of axons. Growth cone advance and navigation requires the activity of their cytoskeletal networks, comprising F-actin in lamellipodia and filopodia as well as dynamic microtubules emanating from bundles of the axonal core. The molecular mechanisms governing these two cytoskeletal networks, their cross-talk, and their response to extracellular signalling cues are only partially understood, hindering our conceptual understanding of how regulated changes in growth cone behaviour are controlled. Here we introduce *Drosophila* growth cones as a suitable model to address these mechanisms. Morphological and cytoskeletal readouts of *Drosophila* growth cones are similar to those of other models, including mammals, as demonstrated here for microtubule and F-actin dynamics, axonal growth rates, filopodial structure and motility, organisational principles of MT networks and subcellular marker localisation. Therefore, we expect fundamental insights gained in *Drosophila* to be translatable into vertebrate biology. The advantage of the *Drosophila* model over others is its enormous amenability to combinatorial genetics as a powerful strategy to address the complexity of regulatory networks governing axonal growth. Thus, using pharmacological and genetic manipulations we demonstrate a role of the actin cytoskeleton in a specific form of microtubule organisation (loop formation), known to regulate growth cone pausing behaviour. We demonstrate these events to be mediated by the actin-microtubule linking factor Short stop, thus identifying an essential molecular player in this context.

**5 key words**: growth cones, cytoskeleton, axons, Drosophila, cell culture

## Introduction

Understanding how neurons wire up into a functional nervous system during development or regeneration is a key challenge for neuroscience research. A crucial process of circuit formation is the guided outgrowth of axons. Axon extension is executed by growth cones (GCs) at their distal tips (Dent and Gertler, 2003; Lowery and Vactor, 2009). GCs are highly dynamic structures characterised by prominent, membranous protrusions comprising finger-like filopodia and veil-like lamellipodia. Filopodia contain rigid bundles of filamentous actin (F-actin), and their exploratory movements are believed to increase the sensory radius of GCs (Mattila and Lappalainen, 2008). Lamellipodia contain lattices of relatively short actin filaments, which drive protrusion of the veil and provide an ideal substrate for myosin to generate the forces that allow GCs to pull (Brown and Bridgman, 2003). Filopodia and lamellipodia are dynamically invaded by individual splayed microtubules (MTs) emanating from the tip of the axonal MT bundle. This invading activity of splayed microtubules is counteracted by the backflowing F-actin networks (Dent and Gertler, 2003; Lee and Suter, 2008). Signals from the extracellular environment can induce stabilisation of splayed MTs in a favoured direction. Subsequent bulk extension of axonal MTs into this area implements GC turning which translates into bent axon extension, i.e. directed growth (Lee and Suter, 2008).

Molecular insights into the machineries regulating and mediating these subcellular events during axon extension have been gradually emerging over recent decades. Thus, we know an impressive number of signalling pathways involved in axonal growth regulation and pathfinding (Huber et al., 2003), and conceptual insights into the molecular machineries regulating F-actin and MT dynamics at growth cones are slowly evolving (Pak et al., 2008; Conde and Caceres, 2009). However, concepts remain highly speculative; they are pieced together from numerous distinct models of axonal growth, built on the premise that insights

can be generalised. More importantly, key questions still remain unanswered. For example, it remains unclear how signalling events involved in pathfinding impinge on the cytoskeletal core machineries to induce predictable changes of growth cone behaviour. Furthermore, we lack insights into the molecular links mediating cross-regulation and coordination of F-actin and MT dynamics during axonal growth. To gain such insights and achieve a more integrated understanding of axon growth mechanisms, research would benefit enormously from growth cone models amenable to combinatorial genetics.

*Drosophila* has a great potential to provide such a platform for research. Building on its genetic potential, many genes and factors with demonstrated requirements for axonal growth *in vivo* have been uncovered and functionally studied in flies; many of these factors are conserved in higher animals (reviewed in Araujo and Tear, 2003; Sánchez-Soriano et al., 2007). Furthermore, an impressive pool of relevant genetic tools is readily available to approach mechanisms of axonal growth experimentally. However, studies in *Drosophila* have mostly been restricted to the analysis of neuronal morphology *in vivo* and little attention has been given to subcellular detail and the study of cytoskeletal dynamics during axonal growth, mainly due to the absence of good *Drosophila* GC models (reviewed in Sánchez-Soriano et al., 2007).

Here we present a GC model based on primary cell cultures generated from *Drosophila* embryos. This model ideally complements *in vivo* work by providing robust readouts for cytoskeletal dynamics in fixed and live cells, all of which can be readily combined with versatile and combinatorial *Drosophila* genetics. The qualitative and quantitative properties of cytoskeletal dynamics revealed by these readouts show striking similarities to descriptions of vertebrate primary neuron models, suggesting a high translational potential of principal insights gained in *Drosophila*. We demonstrate the experimental amenability of the fly model using pharmacological and genetic manipulations of Rac GTPases, F-actin regulators and the cytoskeletal linker molecule Short stop and demonstrate novel insights into the molecular links between F-actin dynamics and the organisation of microtubule networks.

## Methods

### Fly strains

The following fly stocks were used: Oregon R wild-type strain; *scabrous-Gal4* (Mlodzik et al., 1990); *elav-Gal4* (Luo et al., 1994); $enabled^{23}$ (Ahern-Djamali et al., 1999) and $enabled^{GC1}$ (Gertler et al., 1995); $chickadee^{221}$ (Verheyen and Cooley, 1994) and *Df(chickadee)* (Wills et al., 1999); $capping\ protein\ ß^{bnd1}$ (Delalle et al., 2005); $twinstar^{110M}$ (Janody and Treisman, 2006) and *Df(2R)or-BR6* (uncovering *twinstar*; www.flybase.org); $Suppressor\ of\ profilin\ 2^{1}$ and $arp66B^{EP3460}$ (Hudson and Cooley, 2002); $daam^{Ex68}$*, Ubi::GFP/*$Y^{Dp(1;Y)Sz280}$*/C(1)DX* (Matusek et al., 2008); $short\ stop^{3}$ (Lee et al., 2000) and $short\ stop^{sf20}$ (Prokop et al., 1998)*; UAS-eb1-GFP* (P. Kolodziej, unpublished); *UAS-shot-LA-GFP* (Shot::GFP) and its derivative *UAS-shot-LC-GFP* (ΔCalp1; Lee and Kolodziej, 2002); $spaghetti\ squash\ (sqh)^{AX3}$*; P[w+ sqh-gfp]*$^{42}$ (in which the transgene is the only source of regulatory light chain; Royou et al., 2002); *UAS-GFP-fascin* (Zanet et al., 2009); $UASp\text{-}Myo10A\text{-}GFP^{30}$ (Liu et al., 2008); dominant negative $UAS\text{-}Rac1^{N17}$ (Luo et al., 1994).

### Generation of primary cell cultures

Primary cell cultures were generated as described previously (Sánchez-Soriano et al., 2005). Fresh Schneider's *Drosophila* medium (Schneider, 1964; Invitrogen) was supplemented with fetal calf serum (20%, non-heat inactivated; Biochrom, AG Seromed, Berlin, Germany), kept

for 3 days in the dark at 26°C. Then 2µg/ml insulin (Sigma, St Louis, MO, USA; aliquots of 10mg/ml $H_2O$, set to pH2 with glacial acetic acid, were stored at -80°C) was added and pH set to 6.8–6.9. The readily prepared culture medium can be aliquoted and stored at -80°C for a maximum of 4 months. Cells were collected with micromanipulator-attached capillaries from stage 11 embryos (6–7 h after egg lay at 25°C) into sterilised centrifuge tubes with Schneider's medium. Either cells were kept for 2-3 days (maternal depletion cultures) or immediately treated for 5 minutes at 37°C with dispersion medium [200 ml contained 30 ml HBSS (Gibco), 3 ml penicillin-streptomycin-solution (Gibco), 0.01g phenyl-thio urea (Sigma), 167 ml distilled water, 0.5 mg/ml Collagenase (Worthington, Cellsystems) and 2mg Dispase (Roche)], washed in Schneider's medium, and eventually dissolved in the final volume of Schneider's medium (5-6 µl/donor embryo). Each change of medium was preceded by 4 minutes of centrifugation at 1200rpm. Cells can also be mechanically dispersed through pipetting up and down with a 100µl pipette, but neurons derived from this procedure display many more filopodia on axons and GCs (data not shown). In both cases, aliquots of 30-40µl of the final cell suspension were transferred to cover slips, aiming at cell densities in the range of 500-2500 cells/$mm^2$. Too low cell densities negatively impact on cell morphology (reduced filopodia number and neurite length), whereas too high densities cause increased cell cluster formation, thus reducing the number of isolated neurons. After transfer of the cell suspension, cover slips were sealed air-tight with vaseline onto special culture chambers (a microscope slide with a 15mm hole glued on top of an intact slide; Dübendorfer and Eichenberger-Glinz, 1980), turned upside-down 90 min later (hanging drop cultures), and further incubated at 26°C.

Experimental manipulations of GCs

To clamp neurons at defined $[Ca^{2+}]_i$ (intracellular free calcium levels) cultures were incubated for 15 minutes at 26°C in 500nM $Ca^{2+}$ buffer (68.24mM NaCl, 21.77mM KCl, 12.23 mM $MgCl_2$, 12.7mM sucrose, 10mM HEPES, 500nM $CaCl_2$, pH 7.1) or 50nM $Ca^{2+}$ buffer (68.24mM NaCl, 21.77mM KCl, 12.23 mM $MgCl_2$, 12.7mM sucrose, 10mM HEPES, 555µM $Ca^{2+}$ , 3mM EGTA, pH 7.1) containing 10µM ionomycin (Sigma; kept as a 10mM stock in DMSO, Sigma). Control buffer (68.24mM NaCl, 21.77mM KCl, 12.23 mM $MgCl_2$, 12.7mM sucrose, 10mM HEPES and 5mM $CaCl_2$, pH7.1) contained corresponding amounts of DMSO; 5mM $[Ca^{2+}]$ of control buffer corresponds to Schneider's medium (Küppers-Munther et al., 2004). For drug treatments, solutions of 200 nM latrunculin A (Biomol International), 20 µM nocodazole (Sigma), 1 or 10 nM taxol (Sigma) were prepared in Schneider's medium from stock solutions in DMSO. For controls, equivalent concentrations of DMSO were diluted in Schneider's medium. Incubation times at 26°C varied as specified in the text.

Immunohistochemistry and documentation

Cultured *Drosophila* neurons were normally analysed 6 hr after plating. They were fixed (20-30 minutes in 4% paraformaldehyde in 0.05 M phosphate buffer, pH 7-7.2), then washed in PBS with 0.1-0.3% Triton X-100 (PBT). Incubation with antibodies was performed in PBT without blocking reagents using: anti-Enabled (5G2; mouse; 1:20, from Developmental Studies Hybridoma Bank, DSHB, University of Iowa, IA, USA; Bashaw et al., 2000), anti-tubulin (clone DMIA, mouse, 1:1000, Sigma), anti-GFP (1:1000, goat, courtesy of Marcos González-Gaitán) , anti-Fasciclin II (clone ID4, mouse, 1:20, DSHB), Cy3 conjugated anti-HRP (goat, 1:100, Jackson Immuno Research), and FITC-, Cy3- or Cy5-conjugated secondary antibodies (1:100 or 200, donkey, Jackson Immuno Research). F-actin was stained with TRITC-, FITC- and Cy5-conjugated Phalloidin (1:100, Sigma). Coverslips with stained neurons were mounted on slides using Vectashield medium (Vector labs).

Documentation, quantification and statistics

Most images were taken using an AxioCam camera mounted on an Olympus BX50WI microscope. Time lapse phase contrast images were acquired on a Delta Vision RT (Applied Precision) restoration microscope using a 100× phase objective. Fluorescent live imaging was carried out on an Axiovert 200M microscope (Carl Zeiss, Inc.) driven by IP Lab software (BD Biosciences). Motoraxonal length measurements *in vivo* were done as describes elsewhere (Bottenberg et al., 2009). Other measurements, such as filopodial length or axon length, were performed in Image J software. All data are shown as mean ± standard error of the mean (SEM), and statistical analyses were carried out in Sigma Stat 3.0 using Mann-Whitney Rank Sum Tests.

## Results and Discussion

Flexible procedures to yield *Drosophila* GCs in primary cell culture

Using cell culture strategies originally designed for the analysis of late neuronal differentiation of *Drosophila* neurons (Küppers et al., 2003; Küppers-Munther et al., 2004; Sánchez-Soriano et al., 2005), we explored their suitability for the study of axonal growth. To this end, cells were removed with glass capillaries from the neurogenic, ventral area of stage 11 embryos (~45% of development; Prokop and Technau, 1993), i.e. at a stage when most neurons are born and have acquired their identity, and axonal growth is about to begin (Campos-Ortega and Hartenstein, 1997). Subsequently, cells were grown in Schneider's medium, which is highly suitable to support early stages of neuronal development (Küppers-Munther et al., 2004). An essential prerequisite for successful analyses of GCs was the presence of a reasonable fraction of isolated single neurons. This outcome was achieved through enzymatic cell dissociation (Sánchez-Soriano et al., 2005) and proper adjustment of cell densities (see Methods).

The period of time in which GCs could be analysed in these cultures was relatively narrow but could be modified through incubation at different temperatures. To this end, the range of temperatures tolerated by the neurons, yielding good results and normal morphology was between 17°C and 26°C (Fig. 1D-H), whereas cells at 12°C tended to adhere less well and display less filopodia (not shown). Heatshock protocols with six 20 min. intervals at 37°C for 3 hours did not cause any obvious morphological aberrations (not shown). The standard temperature used for most experiments was 26°C. At this temperature, GCs of primary neurons were best analysed at 6-8hr. Already at this stage, occasional puncta of the presynaptic differentiation marker Synapsin could be detected at GCs (Fig. 1A), as likewise reported for growth cones of rat hippocampal neurons (Bonanomi et al., 2005). It is tempting to speculate that these Synapsin puncta represent the vesicular equivalent to quantal release of acyetylcholine measured at *Drosophila* growth cones (Yao et al., 2000). At 15hr after plating neurons had started to adopt mature morphology, in agreement with previous descriptions (Fig. 1B,C; Küppers-Munther et al., 2004; Sánchez-Soriano et al., 2005). The window of GC analysis could be shifted to 15-20hr after plating, if cells were reared at 17°C, whereas cells at 12°C needed more than 25hrs to reach axon lengths comparable to cultures kept under standard conditions (6 hrs at 26°C). In addition to providing more flexibility with respect to experimental timing, incubation at different temperatures provided a strategy to adjust the activity of the Gal4/UAS system for targeted gene expression, which is known to be influenced by temperature (Duffy, 2002).

In order to achieve targeted gene expression, cultures were obtained from embryos carrying a combination of *sca-Gal4* and the respective UAS-construct; in contrast to other pan-

neuronal driver lines (such as *elav-Gal4*), *sca-Gal4* achieved excellent penetrance at this early developmental stage, as judged from strong expression of GFP-tagged factors in most, if not all neurons (see below). Finally, cells removed from embryos could be kept for at least 3 days in a centrifuge tube, before being dispersed and plated. Neurons in these delayed cultures displayed normal morphology (Fig. 1I; Matusek et al., 2008), although they were likely to execute regenerative growth. This finding was in agreement with observations for rat primary cortical neurons, where morphology, motility, and cytoskeletal composition were found to be highly homologous between regenerating and developing neurites (Chuckowree and Vickers, 2003). Importantly, the delayed plating of primary neurons is a quick and invaluable procedure to reduce potential maternal product (gene product deposited during oogenesis) from these neurons. Delayed plating is therefore a feasible procedure that can be used in those cases where germline clones (the standard technique to suppress maternal product deposition; Theodosiou and Xu, 1998) fail to give rise to cellularised embryos.

Taken together, using the procedures outlined above, *Drosophila* GCs can be generated efficiently and allow rapid experimentation a few hours after plating. Since neurons are grown from *Drosophila* embryos, they can be manipulated genetically with the breadth of strategies and tools available for this developmental stage (Sánchez-Soriano et al., 2007) - including targeted construct expression (of genes, markers or iRNA), mutations (zygotic and/or germ line clones), or any feasible combinations of these.

Consistent parameters of MT organisation and dynamics

GCs of *Drosophila* embryonic primary neurons in culture look very similar in shape to GCs of embryonic *Drosophila* motorneurons *in vivo*, and consisted of widened or pointed axonal endings surrounded by filopodia, of which the longer filopodia measured 10-15µm in length (as compared to ≥12µm *in vivo*; Murray et al., 1998; Sánchez-Soriano and Prokop, 2005). Two main types of GCs could be classified in culture, as judged from F-actin staining, the “pointed” and the "laminar" type, which occur in reproducible distributions; pointed GCs are characterised by the absence of prominent lamellipodia and the presence of filopodia, whereas laminar GCs are broad and display filopodia and extensive lamellipodia (Fig. 1). When assessing microtubules by staining against tubulin, three main classes of GCs were found (Fig. 1): the bundled type (blunt or pointed MTs at the axon tip), the looped type (bundled MTs at the axon tip display a curved or looped constellation), and the spread type (GCs contain dispersed arrangements of unbundled, curved MTs). The same classes were described for mouse cortical neurons (Teng et al., 2001), and their relative frequency was surprisingly similar (Fig.1K; Tab.1).

MT networks are organised through different classes of MT-binding proteins, of which plus end tracking proteins (+TIPs) associate with growing MT plus ends and are essential regulators of MT de-/polymerisation processes. *Vice versa*, fluorescently tagged +TIPs provide excellent readouts for MT dynamics (Komarova et al., 2002; Morrison, 2007; Akhmanova and Steinmetz, 2008). When expressing the +TIP EB1::GFP in *Drosophila* primary neurons, highly dynamic comet-like puncta (comets) could be seen moving antero- and retrogradely along the axon and throughout GCs, occasionally extending into filopodia (Fig. 2A; Suppl. Movie). The quantification of anterograde and retrograde movements of EB1 comets in *Drosophila* primary neurons was in good agreement with descriptions for vertebrate neurons (Tab. 1), suggesting that principal regulatory mechanisms of MT dynamics are comparable in both systems.

We conclude that the subcellular organisation and dynamics of MTs in embryonic *Drosophila* primary neurons can be used as experimental readouts; they are in good quantitative and qualitative agreement with parameters described for vertebrate GC models.

Consistent parameters for filopodial actin dynamics

Numbers, lengths and dynamics of filopodia represent easily accessible readouts for studying aspects of F-actin dynamics (e.g. Brown et al., 2000; Gehler et al., 2004). Filopodia of *Drosophila* primary neurons imaged via phase contrast live microscopy displayed the classical features, such as kinking, horizontal drift, protrusion and retraction (Fig. 3; Suppl. Movie). Also cases of engorgement were observed, in which filopodia expand and give rise to the new axon (Fig. 3E; Suppl. Mov.). Similar processes of neurite extension were described for *Drosophila* motorneurons *in vivo* or rat primary neurons in culture (Argiro et al., 1985; Murray et al., 1998). Rates of filopodial protrusion and retraction were in the range of 5-7µm/min, comparable to those reported for mammalian neurons, or data published for *Drosophila* motorneurons *in vivo* (Tab.1). In fixed preparations of primary *Drosophila* neurons measurements of filopodial numbers (7.5 per neurite) and lengths (3-4µm) matched the outcome of live analyses and data published for cultured vertebrate neurons (Fig. 3F,G, Tab.1). Work in other GC models demonstrated a dependency of filopodial dynamics on $[Ca^{2+}]_i$ (levels of intracellular free calcium; Henley and Poo, 2004). In agreement, we found filopodia of *Drosophila* GCs to be reduced in number and severely increased in length at elevated levels of $[Ca^{2+}]_i$ (15 min. at 500nM), whereas both filopodial length and number were reduced at estimated resting levels of $[Ca^{2+}]_i$ (15 min. at 50nM; Henley and Poo, 2004; Fig.4). Together with published reports that GCs of *Drosophila* primary neurons display intrinsic alterations in $[Ca^{2+}]_i$ (Van Berkum and Goodman, 1995; Berke et al., 2006), we conclude that calcium-mediated responses contribute to their F-actin dynamics and growth behaviour.

Also localisation patterns and dynamics of subcellular markers in filopodia were in agreement with other GC models. First, the F-actin barbed end-binding factor Enabled showed a dotted localisation along filopodial shafts and prominent spots at filopodial tips (Fig.4), as previously described for Enabled/VASP in mouse neurons (Lanier et al., 1999). Second, targeted expression of a GFP-tagged version of the F-actin bundling factor fascin was strongly enriched in filopodia, as expected from work in other GC models (Fig.4; Sasaki et al., 1996). Third, a prominent feature of filopodial and lamellipodial dynamics is the backflow of their F-actin networks (Bray and White, 1988; Lin et al., 1996). Myosin II can be used as a marker in filopodia, since it integrates passively into back-flowing F-actin bundles (Rochlin et al., 1995; Brown and Bridgman, 2003). In primary *Drosophila* neurons, a GFP-tagged version of the regulatory light chain of *Drosophila* myosin II (Spaghetti squash; Sqh::GFP; Royou et al., 2002) produced fluorescent puncta which appeared in filopodia and moved centripetally (Fig.2; Suppl. Mov.). The spontaneous occurrence of Sqh::GFP puncta in the GC periphery was in agreement with descriptions in non-neuronal cells (Verkhovsky et al., 1995; Svitkina et al., 1997), and flow rates of 5.5µm/min observed with Sqh::GFP matched descriptions for filopodia of mouse neurons (Tab.1). Also more stable accumulations of Sqh::GFP observed at the base of filopodia (Fig.4; Suppl. Mov.) were similarly described for mammalian GCs (Rochlin et al., 1995; Brown and Bridgman, 2003). Fourth, also the unconventional MyTH4-FERM myosin X localises to and regulates filopodia (Bohil et al., 2006). Its closest relative in *Drosophila* is believed to be the myosin XV homologue Sisyphus, which localises to filopodia in non-neuronal cells (Liu et al., 2008). GFP-tagged Sisyphus likewise localised to filopodia of *Drosophila* primary neurons (Fig.4). Finally, MT invasion of filopodia is a typical feature observed in GCs (Sánchez-Soriano et al., 2007; Lowery and Vactor, 2009); independent of GC class, about a quarter of filopodia was invaded by MTs in *Drosophila* neurons (25±1.45%, n=78 cells; Fig.4).

We conclude that readouts for the subcellular organisation and dynamics of filopodia in embryonic *Drosophila* primary neurons are in good agreement with descriptions for vertebrate or other invertebrate GC models in culture.

Using axonal net growth rate as readout

Measurement of axon length over time is an important readout reflecting the net activity of the axon elongation machinery. Axonal length of *Drosophila* embryonic primary neurons represented a stable readout, equating to an average net growth rate of 3µm/hr (Fig.5), comparable to published values for vertebrate neurons (Tab.1). The core machinery of axon extension is believed to depend on the dynamics of MT but not F-actin networks (see Introduction). In agreement with this notion, application of the MT stabilising drug taxol to *Drosophila* primary neurons for 4hr caused axon shortening in a dose-dependent manner, whereas the F-actin destabilising drug cytochalasin D had no negative impact (Fig.5). These findings are in full agreement with observations made on vertebrate primary neurons (Letourneau and Ressler, 1984; Marsh and Letourneau, 1984; Dent and Gertler, 2003). Interestingly, the reduced axon length phenotype of taxol-treated *Drosophila* neurons was partially rescued when cytochalasin D was co-applied (Fig.5), as was similarly observed in chick primary dorsal root ganglion neurons (Letourneau et al., 1987). Taken together, these data further support the notion that principal mechanisms of cytoskeletal dynamics are conserved between vertebrate and *Drosophila* neurons.

Whereas cytochalasin D has no negative effect on axon growth in culture (Fig.5), its application in *Drosophila* or *Xenopus* embryos *in vivo* was reported to cause axonal bypass and stall phenotypes (Bentley and Toroian-Raymond, 1986; Chien et al., 1993; Kaufmann et al., 1998). Therefore, manipulations of the F-actin cytoskeleton might affect axonal growth in different ways in culture and *in vivo*. To test this possibility genetically, we analysed axonal extension in culture versus *in vivo* of neurons carrying loss-of-function mutations for key actin regulators (profilin, enabled, capping protein, Arp2/3 complex components, the formin Daam, cofilin and Rac GTPases). All deviations from normal axon length revealed in these experiments consistently represented shortening *in vivo*, but lengthening in culture (Fig.6).

We propose that such a differential (i.e. *in vivo* versus culture) axonal growth phenotype, reflects aberrant mechanisms underlying pathfinding, but argues against defects of the core machinery of axon extension. In support of this notion, GCs with impaired F-actin networks have been shown to lose their ability to change direction, i.e. they fail to turn towards off-track attractive cues (resulting in bypass; Lin and Forscher, 1995) and lack the ability to turn away from repulsive cues (resulting in stall; Challacombe et al., 1996). In a standard cell culture model no pathfinding is required, rendering turning behaviour irrelevant. Therefore, in culture, F-actin dynamics add friction to a growing axon, rather than assist the core machinery of axon extension (Pak et al., 2008; Conde and Caceres, 2009). This core machinery depends essentially on MTs, as nicely demonstrated by the axonal stall phenotypes in culture observed upon taxol application (Fig.5; see also Sánchez-Soriano et al., 2009). We conclude that our culture system can be used as a tool to classify axonal growth phenotypes and assign the underlying mechanisms to pathfinding or axonal extension machineries.

Proof of principle: integrating F-actin- and MT-associated mechanisms at GCs

To gain a better understanding of how F-actin dynamics antagonise processes of axon extension in cultured neurons, we analysed the effects of F-actin manipulation on the MT organisation of neurons. To this end we used neurons treated with latrunculin A, expressing dominant negative $Rac^{N17}$, or lacking endogenous functions of enabled or profilin, all of which displayed longer axons in culture (Fig.6). At the subcellular level, their axon length phenotypes clearly correlated with a change in MT organisation at their GCs; bundled MTs were strongly increased, and looped MT constellations drastically reduced (Fig.7A-E). MT loops at GCs are

believed to represent states of pausing (Dent et al., 1999), and could therefore partially explain the extended axon phenotype of the analysed neurons. To test this hypothesis, we set out to identify factors directly involved in loop formation. Two sets of experiments indicated that the MT-binding factor Short stop (Shot; Röper et al., 2002) is such a factor. First, looped MT conformations were completely abolished in *shot* mutant neurons (Fig.7K). Second, the fraction of neurons displaying loops was significantly increased when expressing a GFP-tagged Shot full length construct in wildtype neurons (Shot-LA::GFP; Fig.7G,K). These Shot-LA::GFP expressing neurons displayed shorter axons (Fig.7F,G), in agreement with the initial hypothesis that the presence of looped MTs slows axon extension.

In addition to MT-interacting capabilities, Shot also harbours F-actin-binding calponin homology domains, i.e. can act as a cytoskeletal linker molecule (Lee and Kolodziej, 2002). Therefore, Shot's function in MT loop formation might depend on F-actin dynamics. Two sets of experiments were carried out to test this hypothesis: First, we manipulated F-actin dynamics in neurons expressing Shot-LA::GFP, either via application of latrunculin A or via co-expression of $DRac^{N17}$. Both treatments severely suppressed Shot::GFP-induced MT loops (Fig.7H,I,K). Second, a GFP-tagged Shot construct lacking F-actin binding capabilities (Shot-LC::GFP; Lee and Kolodziej, 2002) was targeted to wildtype neurons. Shot-LC::GFP failed to induce surplus MT loops (Fig.7J,K), although this construct was shown to be functional in other cellular contexts (Bottenberg et al., 2009). Both sets of data strongly suggest that Shot function in MT loop formation depends on the presence of and direct interaction with a properly organised F-actin network. Furthermore, these experiments nicely demonstrate that combinatorial genetics can be used in *Drosophila* primary neurons to gain insights into the systemic integration of distinct molecular mechanisms.

Conclusions and perspectives

The *Drosophila* primary neuronal culture model provides a promising new opportunity for the study of axonal growth mechanisms. All data presented here strongly suggest that the fundamental mechanisms of axonal growth are conserved between *Drosophila* neurons and those of mammals and other vertebrates (Tab.1). This notion gains genetic support from our recent studies on the conserved functions of *Drosophila* Shot and its close mouse homologue ACF7 in axonal growth (Sánchez-Soriano et al., 2009). As a clear advantage over vertebrate or mammalian models of axonal growth, *Drosophila* primary neurons are highly amenable to combinatorial genetics (e.g. Fig.7I), introducing this experimental approach as a routine strategy to the field. Furthermore, data obtained in *Drosophila* primary neurons can be easily compared to *in vivo* analyses (Fig.6), thus delivering additional levels of information. Through these properties, *Drosophila* primary neurons represent a valuable complement to existing growth cone models.

One area to be explored in the forthcoming years will be the use of extracellular signals (extracellular matrix, pathfinding cues) in combination with *Drosophila* primary neurons to unravel the mechanisms which translate signalling into changes of GC behaviour. The principal feasibility of this avenue of research has already been demonstrated in *Drosophila* neuronal cultures (Takagi et al., 1996; Forni et al., 2004), and can now be analysed with the refined readouts reported here.

**References**

Ahern-Djamali SM, Bachmann C, Hua P, Reddy SK, Kastenmeier AS, Walter U, Hoffmann FM. 1999. Identification of profilin and src homology 3 domains as binding partners for *Drosophila* enabled. Proc Natl Acad Sci U S A 96:4977-4982.

Akhmanova A, Steinmetz MO. 2008. Tracking the ends: a dynamic protein network controls the fate of microtubule tips. Nat Rev Mol Cell Biol 9:309-322.
Araujo SJ, Tear G. 2003. Axon guidance mechanisms and molecules: lessons from invertebrates. Nat Rev Neurosci 4:910-922.
Argiro V, Bunge MB, Johnson MI. 1985. A quantitative study of growth cone filopodial extension. J Neurosci Res 13:149-162.
Bashaw GJ, Kidd T, Murray D, Pawson T, Goodman CS. 2000. Repulsive axon guidance: Abelson and Enabled play opposing roles downstream of the roundabout receptor. Cell 101:703-715.
Bentley D, Toroian-Raymond A. 1986. Disoriented pathfinding by pioneer neurone growth cones deprived of filopodia by cytochalasin treatment. Nature 323:712-715.
Berke BA, Lee J, Peng IF, Wu CF. 2006. Sub-cellular $Ca^{2+}$ dynamics affected by voltage- and $Ca^{2+}$-gated $K^{+}$ channels: Regulation of the soma-growth cone disparity and the quiescent state in *Drosophila* neurons. Neuroscience 142:629-644.
Bohil AB, Robertson BW, Cheney RE. 2006. Myosin-X is a molecular motor that functions in filopodia formation. Proc Natl Acad Sci U S A 103:12411-12416.
Bonanomi D, Menegon A, Miccio A, Ferrari G, Corradi A, Kao HT, Benfenati F, Valtorta F. 2005. Phosphorylation of synapsin I by cAMP-dependent protein kinase controls synaptic vesicle dynamics in developing neurons. J Neurosci 25:7299-7308.
Bottenberg W, Sánchez-Soriano N, Alves-Silva J, Hahn I, Mende M, Prokop A. 2009. Context-specific requirements of functional domains of the Spectraplakin Short stop *in vivo*. Mech Dev 126:489-502.
Bray D, White JG. 1988. Cortical flow in animal cells. Science 239:883-888.
Brown J, Bridgman PC. 2003. Role of myosin II in axon outgrowth. J Histochem Cytochem 51:421-428.
Brown MD, Cornejo BJ, Kuhn TB, Bamburg JR. 2000. Cdc42 stimulates neurite outgrowth and formation of growth cone filopodia and lamellipodia. J. Neurobiol. 43:352-364.
Brown ME, Bridgman PC. 2003. Retrograde flow rate is increased in growth cones from myosin IIB knockout mice. J Cell Sci 116:1087-1094.
Campos-Ortega JA, Hartenstein V. 1997. The embryonic development of *Drosophila melanogaster*. Berlin: Springer Verlag. 227.
Challacombe JF, Snow DM, Letourneau PC. 1996. Actin filament bundles are required for microtubule reorientation during growth cone turning to avoid an inhibitory guidance cue. J Cell Sci 109 ( Pt 8):2031-2040.
Chien CB, Rosenthal DE, Harris WA, Holt CE. 1993. Navigational errors made by growth cones without filopodia in the embryonic Xenopus brain. Neuron 11:237-251.
Chuckowree JA, Vickers JC. 2003. Cytoskeletal and morphological alterations underlying axonal sprouting after localized transection of cortical neuron axons *in vitro*. J Neurosci 23:3715-3725.
Conde C, Caceres A. 2009. Microtubule assembly, organization and dynamics in axons and dendrites. Nat Rev Neurosci 10:319-332.
Delalle I, Pfleger CM, Buff E, Lueras P, Hariharan IK. 2005. Mutations in the *Drosophila* orthologs of the F-actin capping protein alpha- and beta-subunits cause actin accumulation and subsequent retinal degeneration. Genetics 171:1757-1765.
Dent EW, Callaway JL, Szebenyi G, Baas PW, Kalil K. 1999. Reorganisation and movement of microtubules in axonal growth cones and developing interstitial branches. J. Neurosci. 19:8894-8908.
Dent EW, Gertler FB. 2003. Cytoskeletal dynamics and transport in growth cone motility and axon guidance. Neuron 40:209-227.

Dübendorfer A, Eichenberger-Glinz S. 1980. Development and metamorphosis of larval and adult tissues of *Drosophila in vitro*. In: Kurstak E, Maramorosch K, Dübendorfer A, Kurstak E, Maramorosch K, Dübendorfer As. Invertebrate systems *in vitro*. Amsterdam: Elsevier North Holland. p 169-185.

Duffy JB. 2002. GAL4 system in *Drosophila*: a fly geneticist's Swiss army knife. Genesis 34:1-15.

Forni JJ, Romani S, Doherty P, Tear G. 2004. Neuroglian and FasciclinII can promote neurite outgrowth via the FGF receptor Heartless. Mol. Cell Neurosci. 26:282-291.

Gehler S, Gallo G, Veien E, Letourneau PC. 2004. p75 neurotrophin receptor signaling regulates growth cone filopodial dynamics through modulating RhoA activity. J Neurosci 24:4363-4372.

Gertler FB, Comer AR, Juang J-L, Ahern SM, Clark MJ, Liebl EC, Hoffmann FM. 1995. *enabled*, a dosage-sensitive suppressor of mutations in the *Drosophila* Abl tyrosine kinase, encodes an Abl substrate with SH3 domain-binding properties. Genes Dev. 9:521-533.

Henley J, Poo MM. 2004. Guiding neuronal growth cones using $Ca^{2+}$ signals. Trends Cell Biol 14:320-330.

Huber AB, Kolodkin AL, Ginty DD, Cloutier JF. 2003. Signaling at the growth cone: ligand-receptor complexes and the control of axon growth and guidance. Annu Rev Neurosci 26:509-563.

Hudson AM, Cooley L. 2002. A subset of dynamic actin rearrangements in *Drosophila* requires the Arp2/3 complex. J Cell Biol 156:677-687.

Janody F, Treisman JE. 2006. Actin capping protein {alpha} maintains vestigial-expressing cells within the *Drosophila* wing disc epithelium. Development 133:3349-3357.

Kaufmann N, Wills ZP, Van Vactor D. 1998. *Drosophila* Rac1 controls motor axon guidance. Development 125:453-461.

Komarova YA, Vorobjev IA, Borisy GG. 2002. Life cycle of MTs: persistent growth in the cell interior, asymmetric transition frequencies and effects of the cell boundary. J Cell Sci 115:3527-3539.

Küppers B, Sánchez-Soriano N, Letzkus J, Technau GM, Prokop A. 2003. In developing *Drosophila* neurones the production of gamma-amino butyric acid is tightly regulated downstream of glutamate decarboxylase translation and can be influenced by calcium. J. Neurochem. 84:939-951.

Küppers-Munther B, Letzkus J, Lüer K, Technau G, Schmidt H, Prokop A. 2004. A new culturing strategy optimises *Drosophila* primary cell cultures for structural and functional analyses. Dev. Biol. 269:459-478.

Lanier LM, Gates MA, Witke W, Menzies AS, Wehman AM, Macklis JD, Kwiatkowski D, Soriano P, Gertler FB. 1999. Mena is required for neurulation and commissure formation. Neuron 22:313-325.

Lee AC, Suter DM. 2008. Quantitative analysis of microtubule dynamics during adhesion-mediated growth cone guidance. Dev Neurobiol 68:1363-1377.

Lee S, Harris K-L, Whitington PM, Kolodziej PA. 2000. *short stop* is allelic to *kakapo*, and encodes rod-like cytoskeletal-associated proteins required for axon extension. J. Neurosci. 20:1096-1108.

Lee S, Kolodziej PA. 2002. Short stop provides an essential link between F-actin and microtubules during axon extension. Development 129:1195-1204.

Letourneau PC, Ressler AH. 1984. Inhibition of neurite initiation and growth by taxol. J Cell Biol 98:1355-1362.

Letourneau PC, Shattuck TA, Ressler AH. 1987. "Pull" and "push" in neurite elongation: observations on the effects of different concentrations of cytochalasin B and taxol. Cell Motil Cytoskeleton 8:193-209.

Lin CH, Espreafico EM, Mooseker MS, Forscher P. 1996. Myosin drives retrograde F-actin flow in neuronal growth cones. Neuron 16:769-782.
Lin CH, Forscher P. 1995. Growth cone advance is inversely proportional to retrograde F-actin flow. Neuron 14:763-771.
Liu R, Woolner S, Johndrow JE, Metzger D, Flores A, Parkhurst SM. 2008. Sisyphus, the *Drosophila* myosin XV homolog, traffics within filopodia transporting key sensory and adhesion cargos. Development 135:53-63.
Lowery LA, Vactor DV. 2009. The trip of the tip: understanding the growth cone machinery. Nat Rev Mol Cell Biol.
Luo L, Liao YJ, Jan LY, Jan YN. 1994. Distinct morphogenetic functions of similar small GTPases: *Drosophila* Drac1 is involved in axonal outgrowth and myoblast fusion. Genes Dev. 8:1787-1802.
Marsh L, Letourneau PC. 1984. Growth of neurites without filopodial or lamellipodial activity in the presence of cytochalasin B. J. Cell Biol. 99:2041-2047.
Mattila PK, Lappalainen P. 2008. Filopodia: molecular architecture and cellular functions. Nat Rev Mol Cell Biol 9:446-454.
Matusek T, Gombos R, Szecsenyi A, Sánchez-Soriano N, Czibula A, Pataki C, Gedai A, Prokop A, Rasko I, Mihaly J. 2008. Formin proteins of the DAAM subfamily play a role during axon growth. J Neurosci 28:13310-13319.
Mlodzik M, Baker NE, Rubin GM. 1990. Isolation and expression of scabrous, a gene regulating neurogenesis in Drosophila. Genes Dev 4:1848-1861.
Morrison EE. 2007. Action and interactions at microtubule ends. Cell Mol Life Sci 64:307-317.
Murray MJ, Merritt D, Brand AH, Whitington PM. 1998. *In vivo* dynamics of axon pathfinding in the *Drosophila* CNS: A time-lapse study of an identified motorneuron. J. Neurobiol. 37:607-621.
Pak CW, Flynn KC, Bamburg JR. 2008. Actin-binding proteins take the reins in growth cones. Nat Rev Neurosci 9:136-147.
Prokop A, Technau GM. 1993. Cell transplantation. In: Hartley D, editor.Hartley Ds. Cellular interactions in development: A practical approach. London New York: Oxford University Press. p 33-57.
Prokop A, Uhler J, Roote J, Bate MC. 1998. The *kakapo* mutation affects terminal arborisation and central dendritic sprouting of *Drosophila* motorneurons. J. Cell Biol. 143:1283-1294.
Rochlin MW, Itoh K, Adelstein RS, Bridgman PC. 1995. Localization of myosin II A and B isoforms in cultured neurons. J Cell Sci 108 ( Pt 12):3661-3670.
Röper K, Gregory SL, Brown NH. 2002. The 'Spectraplakins': cytoskeletal giants with characteristics of both spectrin and plakin families. J. Cell Sci. 115:4215-4225.
Royou A, Sullivan W, Karess R. 2002. Cortical recruitment of nonmuscle myosin II in early syncytial *Drosophila* embryos: its role in nuclear axial expansion and its regulation by Cdc2 activity. J Cell Biol 158:127-137.
Sánchez-Soriano N, Löhr R, Bottenberg W, Haessler U, Kerassoviti A, Knust E, Fiala A, Prokop A. 2005. Are dendrites in *Drosophila* homologous to vertebrate dendrites? Dev. Biol. 288:126-138.
Sánchez-Soriano N, Prokop A. 2005. The influence of pioneer neurons on a growing motor nerve in *Drosophila* requires the neural cell adhesion molecule homolog FasciclinII. J. Neurosci. 25:78-87.
Sánchez-Soriano N, Tear G, Whitington P, Prokop A. 2007. *Drosophila* as a genetic and cellular model for studies on axonal growth. Neural Develop 2:9.

Sánchez-Soriano N, Travis M, Dajas-Bailador F, Goncalves-Pimentel C, Whitmarsh AJ, Prokop A. 2009. Mouse ACF7 and *Drosophila* Short stop modulate filopodia formation and microtubule organisation during neuronal growth. J Cell Sci 122:2534-2542.

Sasaki Y, Hayashi K, Shirao T, Ishikawa R, Kohama K. 1996. Inhibition by drebrin of the actin-bundling activity of brain fascin, a protein localized in filopodia of growth cones. J Neurochem 66:980-988.

Schneider I. 1964. Differentiation of larval *Drosophila* eye-antennal discs *in vitro*. J. Exp. Zool. 156:91-104.

Svitkina TM, Verkhovsky AB, McQuade KM, Borisy GG. 1997. Analysis of the actin-myosin II system in fish epidermal keratocytes: mechanism of cell body translocation. J Cell Biol 139:397-415.

Takagi Y, Nomizu M, Gullberg D, MacKrell AJ, Keene DR, Yamada Y, Fessler JH. 1996. Conserved neuron promoting activity in *Drosophila* and vertebrate laminin alpha1. J. Biol. Chem. 271:18074-18081.

Teng J, Takei Y, Harada A, Nakata T, Chen J, Hirokawa N. 2001. Synergistic effects of MAP2 and MAP1B knockout in neuronal migration, dendritic outgrowth, and microtubule organization. J. Cell Biol. 155:65-76.

Theodosiou NA, Xu T. 1998. Use of FLP/FRT system to study *Drosophila* development. Methods 14:355-365.

Van Berkum MF, Goodman CS. 1995. Targeted disruption of $Ca^{2+}$-calmodulin signaling in *Drosophila* growth cones leads to stalls in axon extension and errors in axon guidance. Neuron 14:43-56.

Verheyen EM, Cooley L. 1994. Profilin mutations disrupt multiple actin-dependent processes during *Drosophila* development. Development 120:717–728.

Verkhovsky AB, Svitkina TM, Borisy GG. 1995. Myosin II filament assemblies in the active lamella of fibroblasts: their morphogenesis and role in the formation of actin filament bundles. J Cell Biol 131:989-1002.

Wills Z, Marr L, Zinn K, Goodman CS, Van Vactor D. 1999. Profilin and the Abl tyrosine kinase are required for motor axon outgrowth in the *Drosophila* embryo. Neuron 22:291-299.

Yao W-D, Rusch J, Poo M-m, Wu C-F. 2000. Spontaneous acetylcholine secretion from developing growth cones of *Drosophila* central neurons in culture: effects of cAMP-pathway mutations. J. Neurosci. 20:2626-2637.

Zanet J, Stramer B, Millard T, Martin P, Payre F, Plaza S. 2009. Fascin is required for blood cell migration during *Drosophila* embryogenesis. Development 136:2557-2565.

## Figures

**Fig.1** GCs of *Drosophila* primary neurons

A-C) Isolated primary neurons after 6hr, 15hr or 48hr in culture, labelled against tubulin (tub), F-actin (act), and the presynaptic markers Synapsin (Syn) or Bruchpilot (Brp); maturing and mature neurons display numerous orphan presynaptic sites (B,C), and first accumulations can occasionally be seen already at GCs (arrow head in A). D-I) Examples of GCs stained for tubulin (green) and F-actin (magenta), after being cultured under different conditions: raised for 6hr at 26°C (D-G, I), 16 hr at 17°C (H), or for 6hr at 26°C after being kept in a centrifuge tube for 3 days at 26°C (I); classification of GCs as pointed or lamellar with bundled, spread or looped MTs is indicated by colour code, as explained in J and K. J) Quantification of different GC classes from 4 independent experiments shows comparable distributions (chi-square tests: $P_{1\text{-}4}$=0.018, $P_{2\text{-}4}$=0.38). K) Quantification of different MT organisational classes from 4 different experiments (chi-square tests: $P_{1\text{-}4}$=0.096); note that

mouse hippocampal primary neurons were reported to show a similar distribution of MT classes (Teng et al., 2001). Scale bar 10µm in A-C, 5µm in D-I.

**Fig.2** Cytoskeletal dynamics in *Drosophila* primary neurons

Sequence of still images showing live dynamics of EB1::GFP (A) and Sqh/myosinII::GFP (B) in *Drosophila* primary neurons (taken from Suppl. Movie). Sequences illustrate anterograde movements of EB1::GFP puncta in axon (curved arrows in A) and filopodium (arrow heads in A), retrograde movements of Sqh::GFP (white arrowheads in B) and static patches of GFP at the base of filopodia (open arrows in B); note that the Sqh::GFP dot in one of the filopodia has not yet appeared in the first image (open arrowhead in B). Scale bar 5µm.

**Fig.3** Filopodial dynamics and quantification

Sequences of time laps images taken at room temperature in standard Schneider's medium, showing extension (arrows in A), retraction (arrowhead in B), lateral drift (from black to white dot in C), kinking (curved arrow in D), and engorgement (curved arrow in E) of filopodia (taken from Suppl. Movie); time points relative to respective first images are given (bottom right). Box-and-whisker plots illustrating distributions of filopodial length (F) and filopodial number (G) in fixed preparations of primary neurons; in each case 4 independent experiments are shown and, for each experiment, the mean ± SEM plus sample number (n) is indicated (pooled mean for filopodial length is 3.14µm ± 0.07SEM, n=590, and for filopodial number is 7.48 filopodia per neurite ± 0.33SEM, n=118). Mann-Whitney rank sum tests indicated data of different experiments to be similar (respective P-values for filopodial length: $P_{1\text{-}2}$=0.166, $P_{1\text{-}3}$=0.383, $P_{1\text{-}4}$=0.063, $P_{2\text{-}3}$=0.503, $P_{2\text{-}4}$=0.767, $P_{3\text{-}4}$=0.283; P-values for filopodial number: $P_{1\text{-}2}$=0.661, $P_{1\text{-}3}$=0.581, $P_{1\text{-}4}$=0.448, $P_{2\text{-}3}$=0.899, $P_{2\text{-}4}$=0.852, $P_{3\text{-}4}$=0.856). Scale bar 5µm.

**Fig.4** Further properties of filopodia

A-C') GCs incubated for 15 min in control solution (A) or at 50nm $[Ca^{2+}]_i$ show no obvious qualitative deviations (B), whereas GCs at 500nm $[Ca^{2+}]_i$ show dramatic elongation of their filopodia (curved arrows in C); in addition, axonal MT bundles display a club-shaped ending (arrow heads in C,C'). D,E) Quantitative analyses (normalised to controls) of calcium-treated cells: filopodial numbers (D) were reduced in both experimental groups, filopodial length (E) was increased at 500nm $[Ca^{2+}]_i$ and slightly reduced at 50nm $[Ca^{2+}]_i$; respective p-values above/in columns indicate significant deviation from controls (Mann-Whitney rank sum tests). F-J') Immunocytochemical and live imaging studies using candidate filopodial markers (boxed areas shown as close-ups): dots of Enabled staining (Ena) were found in shafts and tips of filopodia in wildtype (close-up in F), but were virtually absent in *enabled* mutant neurons (close-up in G) which displayed dramatically reduced filopodia; live imaging of fascin::GFP (fascin)-expressing neurons revealed strong enrichment along filopodia (curved arrows in H); anti-GFP labelled dots of Sisyphus/myosinXV::GFP (Sys) localised along filopodia (close-up in I); a fraction of filopodia contained splayed microtubules (curved arrows in J,J'); magenta staining throughout represents phalloidin staining. Scale bar 10µm in A-C', 5µm in F-J'; insets are magnified twofold.

**Fig.5** Using axon length as readout for the analysis of axonal growth

A) Box-and-whisker plots illustrating the distribution of axon lengths after 6hr in culture at 26°C; four independent experiments are plotted, respective means ± SEM and sample numbers (n) are given for each experiment; pooled data (n=163): 3.05µm/hr ± 0.08 SEM, 18.29µm ± 0.46 SEM; Mann-Whitney rank sum tests indicated samples to be similar

(respective P-values: $P_{1-2} = 0.661$, $P_{1-3} = 0.581$, $P_{1-4} = 0.448$, $P_{2-3} = 0.899$, $P_{2-4}=0.852$, $P_{3-4} = 0.856$). B-E) Examples of neurons treated for 4hr with control solution (DMSO), 0.4ug/ml cytochalasin D (CytD), 40nm taxol or a combinations of both drugs; tubulin in green, F-actin in magenta, arrowheads indicate tips of axons, asterisks the cell bodies. F) Bar diagram showing the quantification results of drug treatments: various concentrations of taxol are indicated, highly significant deviations are marked with asterisks as determined by Mann-Whitney rank sum tests (respective P values: $P_{1-2} = 0.912$, $P_{1-3}=0.004$, $P_{1-4}=0.001$, $P_{1-5}<0.001$, $P_{1-6}=0.015$, $P_{5-6}<0.001$). Scale bar 10µm.

**Fig.6** Genetic manipulations of actin regulators cause opposite effects on axon length *in vivo* and in culture

A,B) Examples of primary neurons derived from wildtype (wt) or profilin-deficient embryos [profilin: *chicadee*$^{221}$*/Df(chic)*]; arrow heads indicate axon tips, tubulin in green, F-actin in magenta. C,D) Examples of motornerves *in vivo* of embryos with the same genotypes as in A,B; arrowheads indicate nerve tips (nerves labelled with anti-FasciclinII in green), asterisks mark anti-HRP-labelled (magenta) cellular landmark in abdominal segments used to quantify nerve extension (Bottenberg et al., 2009); dots indicate equivalent structures in thoracic segments. E) Quantification of motornerve length *in vivo* (blue) and axon length in culture (red); all data were normalised to wildtype controls; genotypes indicated below the graph: *Drosophila* profilin loss of function (as in B,D), *enabled*$^{23/GC1}$, *capping protein ß*$^{bnd1}$, targeted expression of Rac$^{N17}$ (see also; Sánchez-Soriano and Prokop, 2005), *Drosophila* Arp3 subunit (*arp66B*$^{EP3640}$), neuronal formin (*daam*$^{ex68/+}$), p40 subunit of Arp2/3 (*sop2*$^{1}$) *Drosophila* cofilin (*twinstar*$^{110M}$*/Df*); P-values (Mann-Whitney Rank sum test) and sample numbers are indicated; for all shown genotypes, independent measurements reveal reduction in filopodial numbers, i.e. aberrations of F-actin networks, only cofilin failed to display any such phenotypes (C.P., N.S.S. and A.P., manuscript in preparation). Scale bar 10µm.

**Fig.7** Integrating mechanisms of F-actin and MT dynamics

A-D) Examples of primary neurons derived from wildtype (A), *enabled*$^{23/23}$ mutant (B), *chickadee*$^{221/P5205}$ mutant (profilin; C) or Rac$^{N17}$-expressing embryos (D); F-actin (act) is shown in magenta and as greyscale insets (i); tubulin (tub) is shown in green and as greyscale insets (ii). E) Manipulations of F-actin networks (latA, 1hr 200nm latrunculin A; enabled, as in B; profilin, as in C) significantly increased bundled organisation of MTs at GCs (compare Fig.1D,E; P-values according to Mann-Whitney Rank sum tests: $P_{1-2}=0.002$, $P_{1-3}=0.001$, $P_{1-4}<0.001$, $P_{1-5}=0.002$; *≤0.05; **≤0.005). F) Targeted expression of Shot-LA in primary neurons causes highly significant shortening of axons (P=0.002, Mann-Whitney Rank sum tests). G-J) Examples of primary neurons with targeted expression of Shot-LA::GFP (G), Shot-LC::GFP (H), and Shot-LA::GFP combined with either 1hr application of 200nm latrunculin A (H) or Rac$^{N17}$-expression (I); F-actin (act) is shown in red and as greyscale insets (i); tubulin (tub) is shown in green and as greyscale insets (ii), GFP is shown in blue and as greyscale insets (iii). K) Manipulations of F-actin networks (as in E) significantly decreased looped organisation of MTs at GCs (compare Fig.1G), whereas Shot-LA::GFP expression increased loops, an effect that is suppressed in combination with latrunculin A or Rac$^{N17}$, and which is not achieved upon Shot-LC::GFP expression; sample numbers n indicate total number of measured neurons (before slash) and number of independent experiments used to determine significance (behind slash); asterisks indicate significance according to Mann-Whitney Rank sum tests (*≤0.05; **≤0.005; black, comparison to wildtype: $P_{1-2}=0.002$, $P_{1-3}=0.005$, $P_{1-4}<0.001$, $P_{1-5}=0.042$, $P_{1-6}\leq0.001$, $P_{1-7}=0.016$, $P_{1-8}=0.056$, $P_{1-9}=0.133$, $P_{1-10}=0.497$; grey, comparison to Shot-LA::GFP: $P_{7-8}=0.016$, $P_{7-9}<0.001$, $P_{7-10}=0.032$; further comparisons: $P_{2-8}=0.177$, $P_{5-9}=0.477$). Scale bar 10µm; insets are not magnified.

**Supplementary Movie:** Cytoskeletal dynamics of *Drosophila* primary neurons

Six film sequences showing different aspects of cytoskeletal and filopodial dynamics. A,A') Two examples of neurons expressing EB1::GFP, visible as moving puncta in axon, growth cone and filopodia (details in Fig.2A). B) Neuron expressing Sqh/myosinII::GFP visible as steady patches at the base of filopodia and backflowing puncta in filopodia (details in Fig.2B). C) Phase contrast movie showing protrusion and retraction (illustrated by black arrowheads tracing filopodial tips) and transient bifurcation (indicated by white arrows) of filopodia (compare Fig.3A). D) Phase contrast movie showing kinking of filopodia (indicated by white arrows; compare Fig.3D). E) Phase contrast movie showing lateral drift of filopodial bases (movements traced by white arrow heads; compare Fig.3C). F) Phase contrast movie showing filopodial engorgement (compare Fig.3E); first curved arrow indicates tip of the axon at start of movie, second curved arrow at the end of the movie.

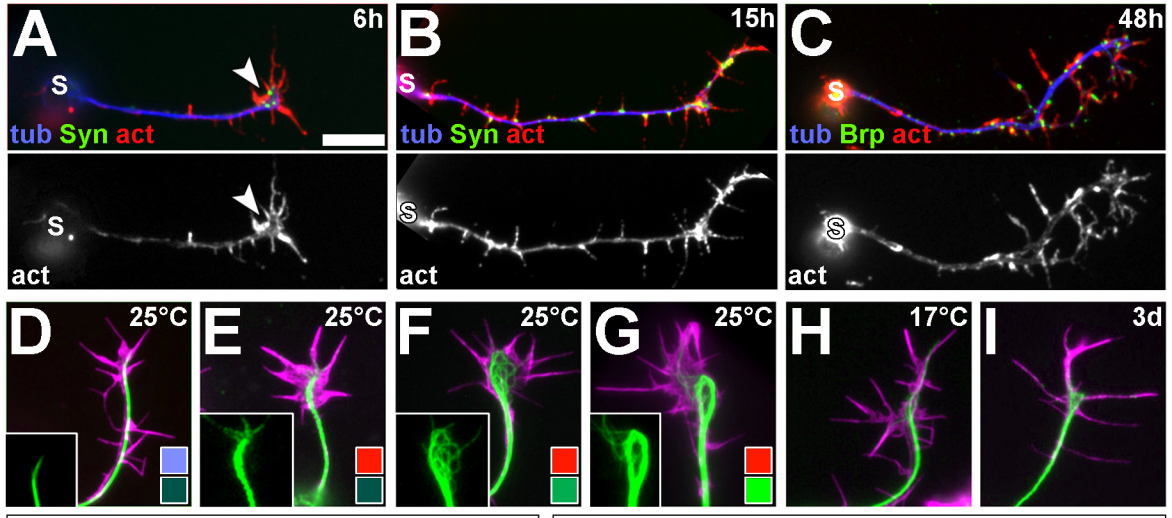


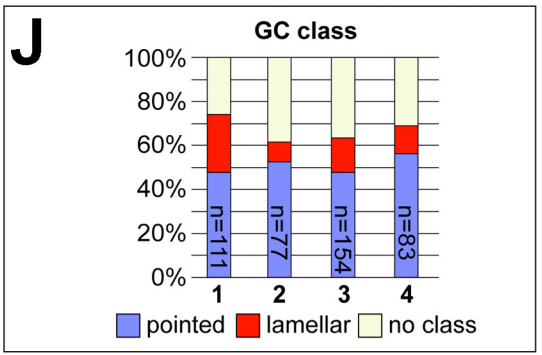


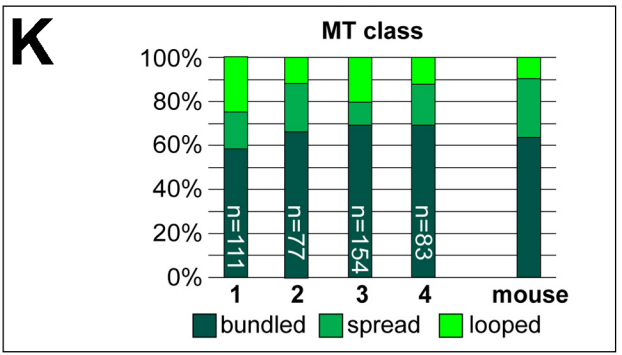


**Fig.1 Sanchez-Soriano et al.**

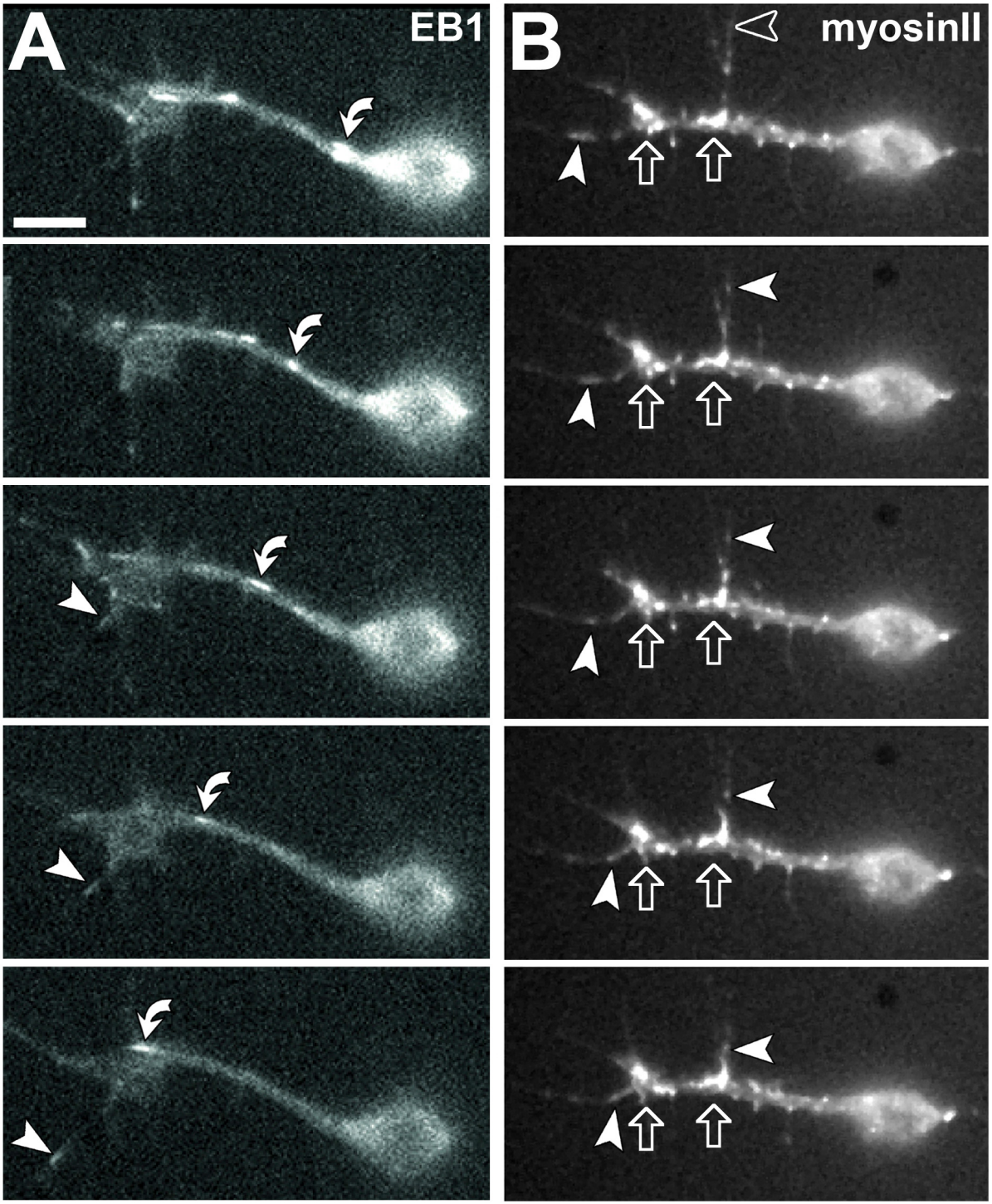


Fig.2 Sanchez-Soriano

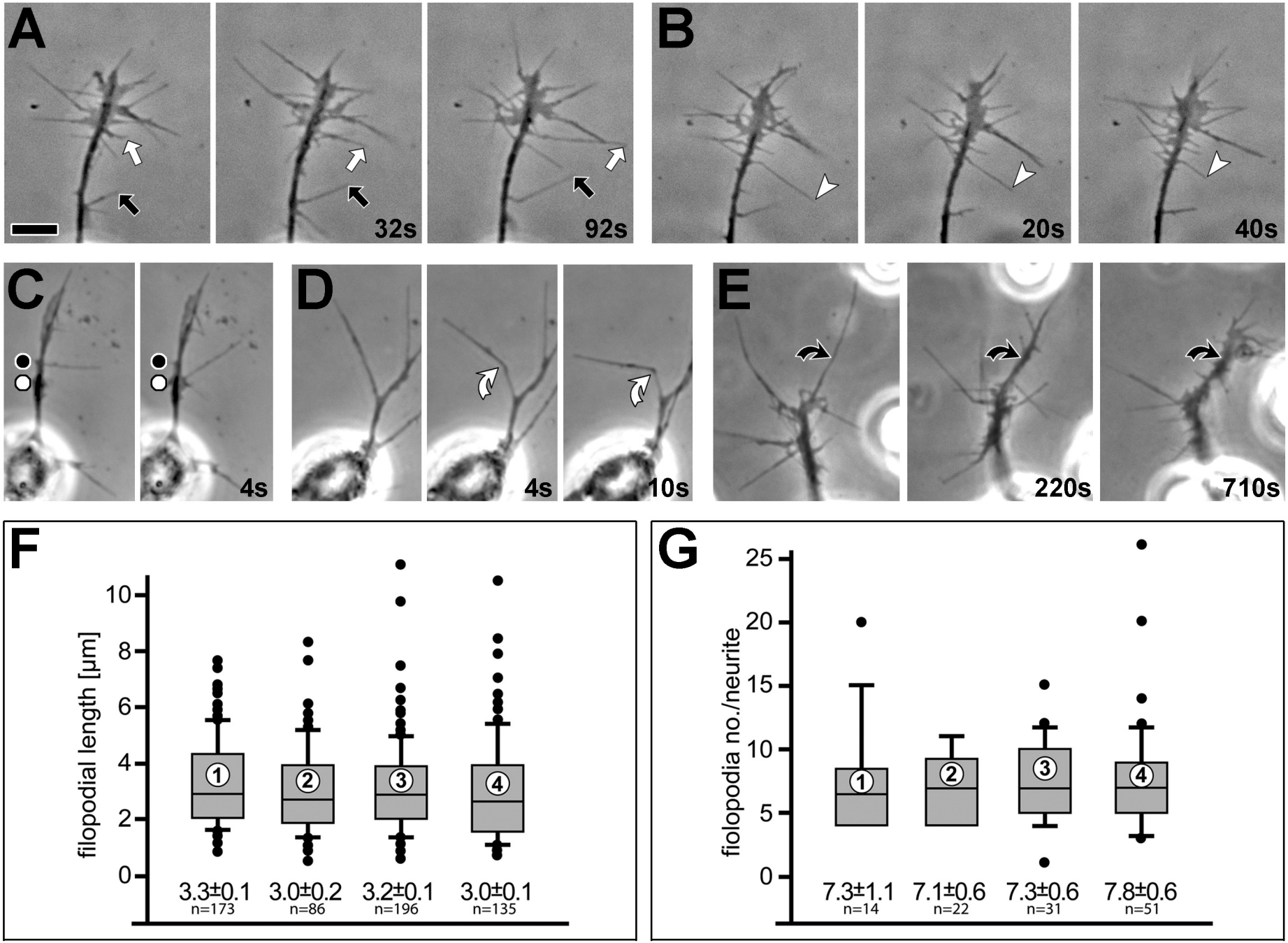


**Fig.3 Sanchez-Soriano et al.**

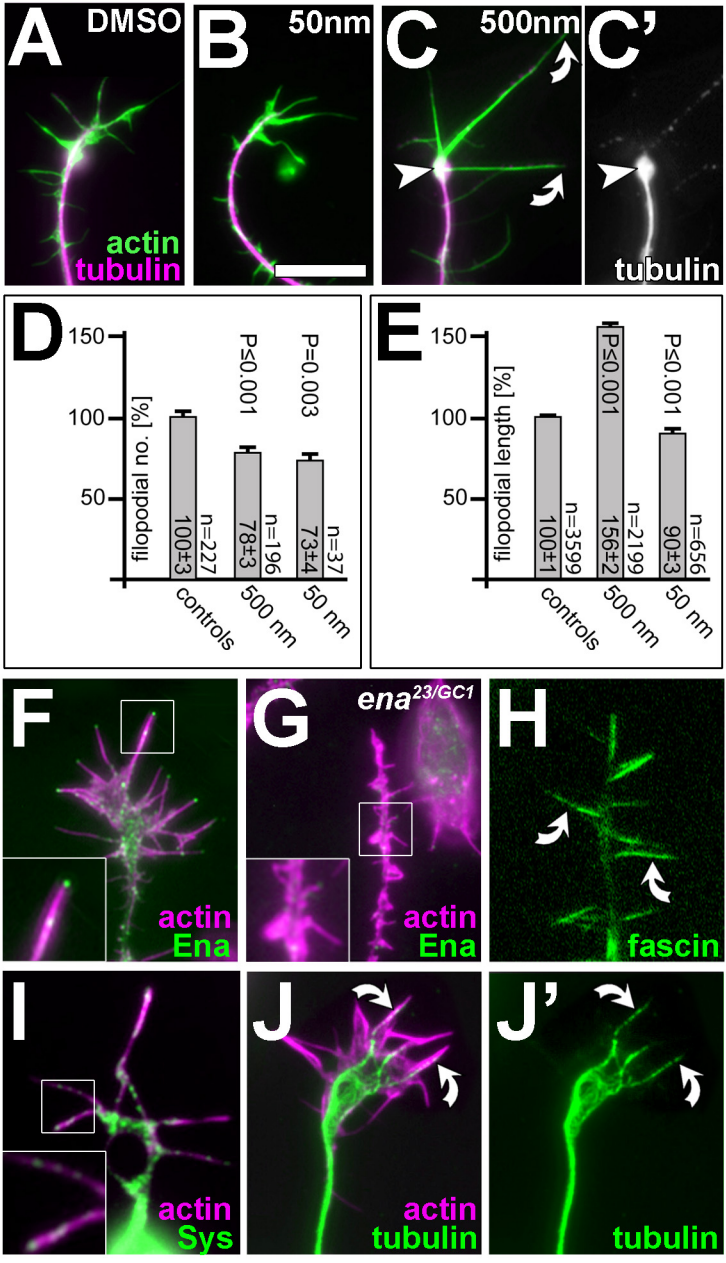


**Fig.4 Sanchez-Soriano et al.**

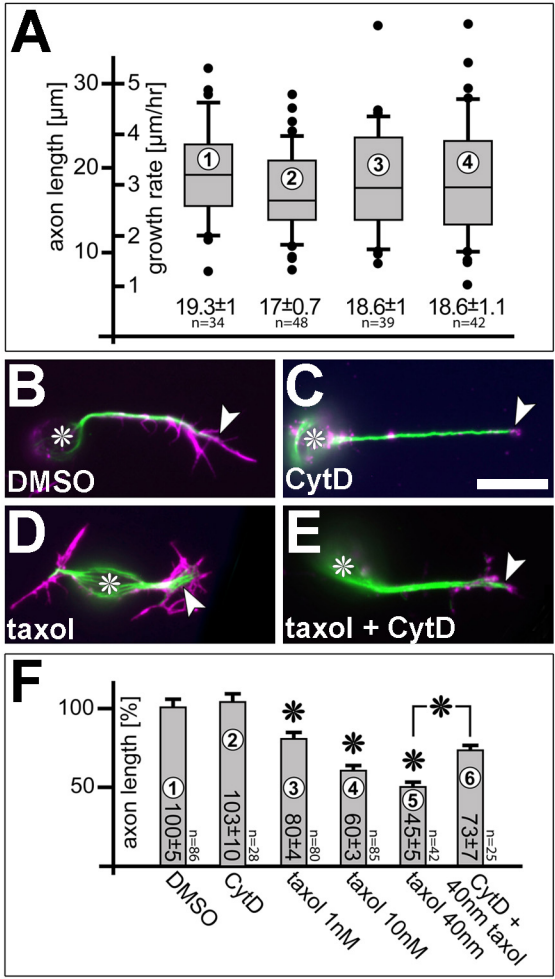


**Fig.5 Sanchez-Soriano et al.**

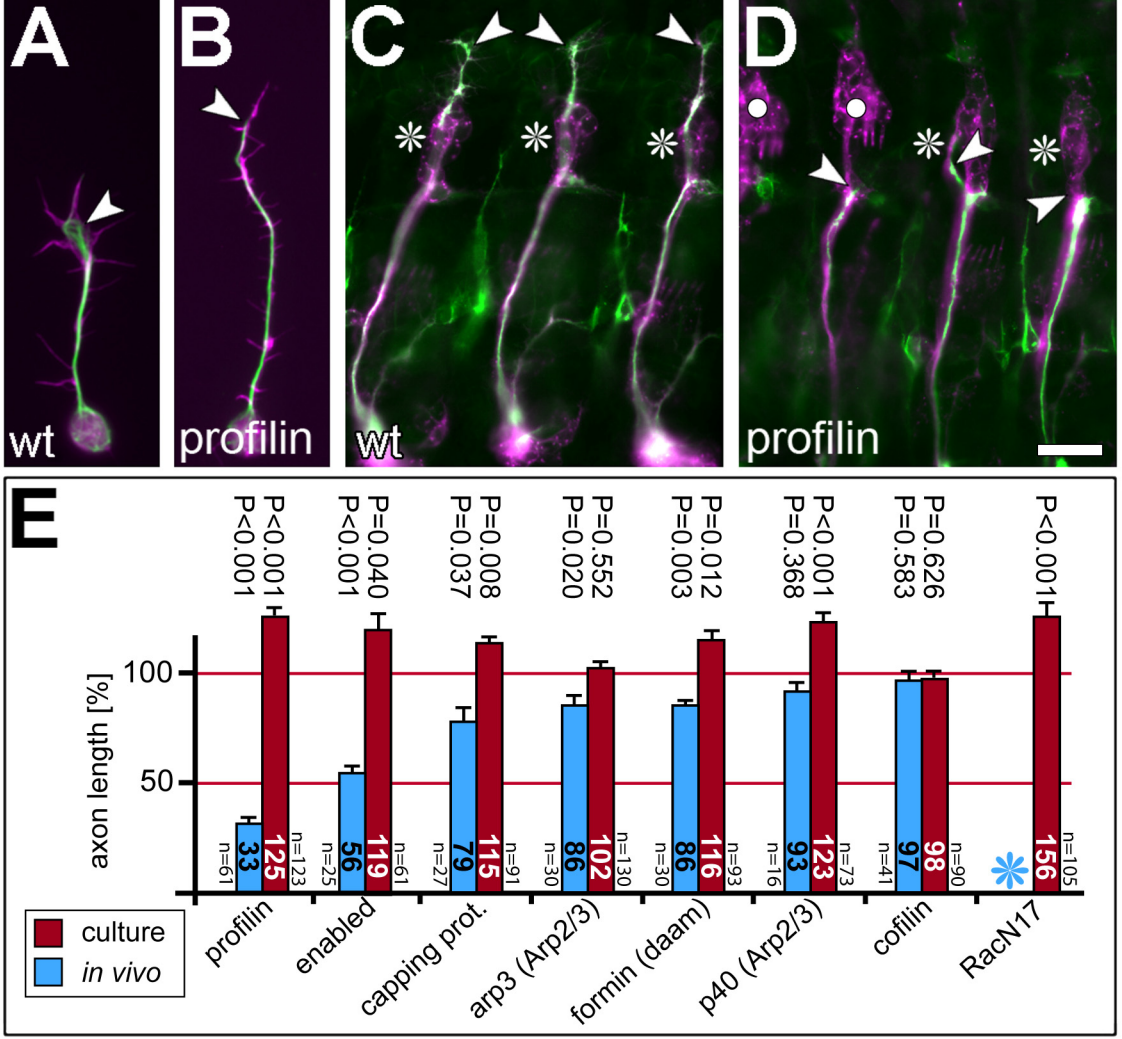


**Fig.6 Sanchez-Soriano et al.**

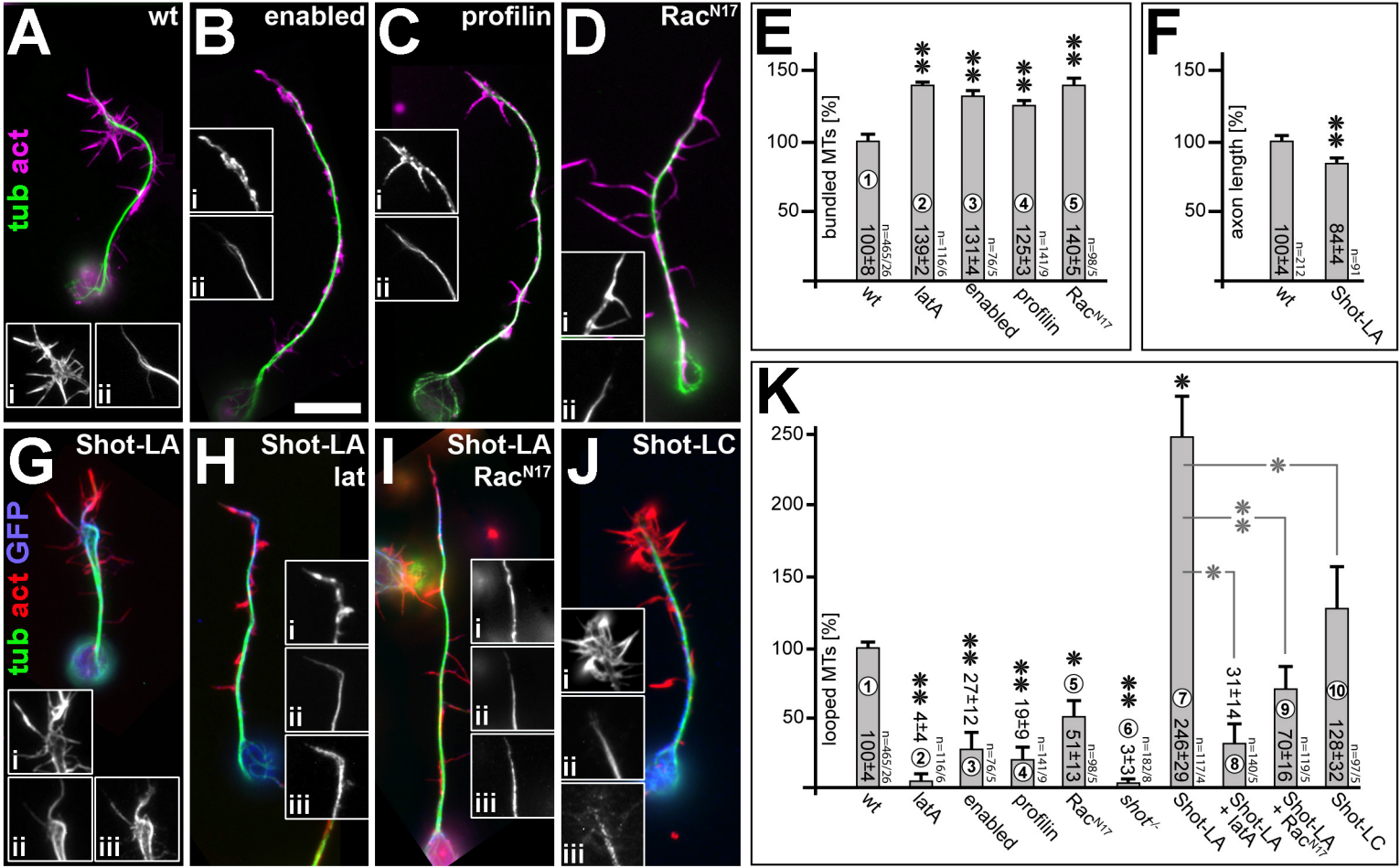


**Fig.7 Sanchez-Soriano et al.**